Diffusion and Subdiffusion of Interacting Particles on Comblike Structures

O. Bénichou, P. Illien, G. Oshanin, A. Sarracino, and R. Voituriez
Sorbonne Universités, UPMC Université Paris 06, UMR 7600, LPTMC, F-75005 Paris, France
and CNRS, UMR 7600, Laboratoire de Physique Théorique de la Matière Condensée, F-75005 Paris, France
(Received 2 July 2015; published 25 November 2015)

We study the dynamics of a tracer particle (TP) on a comb lattice populated by randomly moving hard-core particles in the dense limit. We first consider the case where the TP is constrained to move on the backbone of the comb only. In the limit of high density of the particles, we present exact analytical results for the cumulants of the TP position, showing a subdiffusive behavior $\sim t^{3/4}$. At longer times, a second regime is observed where standard diffusion is recovered, with a surprising nonanalytical dependence of the diffusion coefficient on the particle density. When the TP is allowed to visit the teeth of the comb, based on a mean-field-like continuous time random walk description, we unveil a rich and complex scenario with several successive subdiffusive regimes, resulting from the coupling between the geometrical constraints of the comb lattice and particle interactions. In this case, remarkably, the presence of hard-core interactions asymptotically speeds up the TP motion along the backbone of the structure.

DOI: 10.1103/PhysRevLett.115.220601 PACS numbers: 05.40.Fb, 02.50.-r

The subdiffusive motion of tracers in crowded media, e.g., biological cells, is widespread. Among the microscopic scenarios producing this sublinear growth with time of the mean square displacement (MSD), geometric constraints related to the complexity of the environment play an important role [1,2]. In this context, the comb model (see Fig. 1), where particles can jump in the x direction only when y is zero, has attracted considerable attention because of its simplicity and ability to reproduce subdiffusive behaviors of disordered systems [3].

Comblike structures were introduced to model diffusion in fractals like percolation clusters, with the backbone and teeth of the comb representing the quasilinear structure and dangling ends of percolation clusters [4]. The particle can spend a long time exploring a tooth, resulting in a subdiffusive motion along the backbone: $\langle x^2(t)\rangle \propto t^\alpha$; $\alpha = 1/2$. Numerous results have since been obtained for this model [5–12], including the determination of the occupation-time statistics [13] and of mean first-passage times between two nodes [14] and the case of fractional Brownian walks [15].

In parallel, the comb model has been invoked to account for transport in real systems like spiny dendrites [11], diffusion of cold atoms [16] and diffusion in crowded media [17]. However, all existing studies focused on single-particle diffusion, and interactions between particles have up to now been completely left aside. As an elementary model of particles under short-range repulsive forces, we consider excluded-volume interactions (EVIs) and focus on their impact on tracer dynamics on comblike structures.

From a theoretical perspective, lattice systems of interacting particles represent a prototypical model that has generated a huge number of works in the physical [18,19] and mathematical literature [20]. The effect of EVIs on *homogeneous* lattices is well known [3]. In dimension $d \geq 2$, tracer diffusion remains normal, with a diffusion coefficient resulting from many-body interactions [21]. In "single-file" geometry, where particles cannot bypass each other, the impact of EVIs is stronger, resulting in a subdiffusive behavior $\langle x^2(t)\rangle \propto t^\beta$, $\beta = 1/2$ [22–27]. In this context, determining the effect of EVIs on systems with *geometrical constraints* appears to be an important question which has not received much attention. Notable exceptions are Ref. [28], where two particles only are involved, Refs. [29–31], which consider single-file models for Brownian and subdiffusive motion, Ref. [32], where mobility in single-file systems was shown to be increased by disorder, and Ref. [33], where tracer diffusion on fractal aggregates was studied numerically and found not to be modified by EVIs. In this Letter, we show that, in contrast, EVIs deeply modify tracer diffusion on comblike structures. Focusing on the high density limit, we show analytically that the dynamics displays several regimes

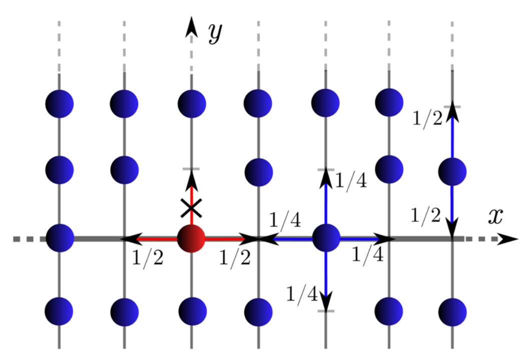

FIG. 1 (color online). Comb model. The x axis is the *backbone*, whereas the orthogonal lines are the *teeth*. Jump rules of the particles in the case when the TP (in red) is restricted to the backbone are given.

of subdiffusion. Surprisingly, EVIs are shown to asymptotically speed up tracer diffusion along the backbone.

Model.—We consider the two-dimensional comb $\mathbf{C}_2$, which is a subgraph of $\mathbb{Z}^2$ obtained by removing all of the lines parallel to the x axis, except for the x axis itself. This lattice is populated by a density ρ of hard-core particles performing nearest-neighbor symmetric random walks. We add a tracer particle (TP) at the origin and focus on its dynamics in the dense limit, where the vacancy density $\rho_0 = 1-\rho \ll 1$. In this limit, it is convenient to follow the vacancy dynamics instead of the dynamics of the particles. We assume that, at each time step, each vacancy exchanges its position with one of the neighboring particles with jump probabilities that depend on the position on the lattice; see the Supplemental Material [34] for their explicit definition.

Case of a TP restricted to the backbone.—We first assume that the TP is constrained to move on the backbone. This particular case is important for several reasons. (i) It mimics the case where the tracer is different from the bath particles, and it cannot visit the teeth. (ii) It appears as an extension of the famous single-file geometry in which, due do the possibility for the bath particles to visit the teeth, the particles can bypass each other. An interesting question is to determine whether the dynamics is still anomalous in this case and, if so, with which exponent. (iii) Finally, solving this auxiliary problem will allow us to determine the dynamics of the TP in the general case where the TP can access the teeth of the comb.

Let X_t be the position of the TP along the backbone at time t, $\kappa^{(n)}(t)$ the cumulants of order n of X_t, and $\Psi_t(k) \equiv \ln\langle e^{ikX_t}\rangle = \ln[\tilde{P}_t(k)]$ the cumulant generating function (CGF). Here, $\tilde{P}_t(k) = \sum_X e^{ikX} P_t(X)$ is the Fourier transform of the probability $P_t(X)$ of finding the TP at position X at time t. Following the method developed in Refs. [37,38] and recently used to study driven diffusion in one-dimensional geometries [39], we first consider the case where there is a single vacancy on the lattice. Let $P_t^{(1)}(X|\mathbf{Z})$ be the probability of finding the TP at position X at time t knowing that the vacancy started from site $\mathbf{Z}$. Summing over all the passages of the vacancy to the TP location, one gets

$$\begin{aligned} P_t^{(1)}(X|\mathbf{Z}) &= \delta_{X,0}\left(1-\sum_{j=0}^{t} F_j(\mathbf{0}|\mathbf{Z})\right) + \sum_{p=1}^{+\infty}\sum_{m_1,m_2,\ldots,m_p=1}^{+\infty} \\ &\times \sum_{m_{p+1}=0}^{+\infty} \delta_{m_1+\ldots+m_{p+1},t}\,\delta_{X,\frac{\sigma(\mathbf{Z})+(-1)^{p+1}}{2}} \\ &\times \left(1-\sum_{j=0}^{m_{p+1}} F_j(\mathbf{0}|\sigma(\mathbf{Z})(-1)^p \mathbf{e}_1)\right) \\ &\times F_{m_p}(\mathbf{0}|\sigma(\mathbf{Z})(-1)^{p+1}\mathbf{e}_1)\ldots F_{m_2}(\mathbf{Z}|-\sigma(\mathbf{Z})\mathbf{e}_1) F_{m_1}(\mathbf{0}|\mathbf{Z}), \end{aligned} \tag{1}$$

where $F_t(\mathbf{0}|\mathbf{Z})$ is the probability for the vacancy to reach the origin for the first time at time t, knowing that it started from site $\mathbf{Z}$, and $\mathbf{e_1}$ is the unit vector in the x direction and $\sigma(\mathbf{Z}) \equiv \mathrm{sgn}(\mathbf{Z}\cdot\mathbf{e}_1)$. The first term on the rhs of Eq. (1) represents the event that, at time t, the TP has not been visited by any vacancy, while the second one results from a partition both on the number of visits p and waiting times m_i between visits of the TP by the vacancy. Computing the generating function associated with this propagator $\hat{p}_{\pm1}(X;\xi) \equiv \hat{P}^{(1)}(X|\pm\boldsymbol{e}_1;\xi)$, where $\hat{\phi}(\xi)$ denotes the discrete Laplace transform $\hat{\phi}(\xi) \equiv \sum_{t=0}^{\infty}\phi_t\xi^t$, and noticing that for symmetry reasons $\hat{F}(\mathbf{0}|\boldsymbol{e}_1;\xi) = \hat{F}(\mathbf{0}|-\boldsymbol{e}_1;\xi) \equiv \hat{F}_1$, one gets

$$\hat{p}_{\pm1}(X;\xi) = \frac{\delta_{X,0}(1-\hat{F}_1) + \delta_{X,\pm1}\hat{F}_1(1-\hat{F}_1)}{(1-\hat{F}_1{}^2)(1-\xi)}. \tag{2}$$

Note that, in that case of a single vacancy, the TP is localized to the sites $0, \pm1$.

We then study the case where the concentration of vacancies ρ_0 is finite but small. We start from a finite lattice of N sites and M vacancies with initial positions $\mathbf{Z}_1, \ldots, \mathbf{Z}_M$, so that $M = \rho_0 N$. The probability $P_t(X|\{\mathbf{Z}_j\})$ to find the TP at position X is given by

$$P_t(X|\{\mathbf{Z}_j\}) = \sum_{Y_1,\cdots,Y_M} \delta_{X,Y_1+\cdots+Y_M} P_t(\{Y_j\}|\{\mathbf{Z}_j\}), \tag{3}$$

where $P_t(\{Y_j\}|\{\mathbf{Z}_j\})$ is the probability that at time t the TP moved a distance Y_j due to its interactions with the jth vacancy. To leading order in ρ_0, the vacancies contribute independently to the displacement of the TP, so that, in Fourier variable, $\tilde{P}_t^{(M)}(k) = [\tilde{P}_t^{(1)}(k)]^M$, where $\tilde{P}_t^{(j)}(k)$ is the Fourier transform of the probability distribution to find the TP at position X at time t, knowing that there are j vacancies on the lattice, and averaged over the initial position of the vacancies, which is assumed to be uniform. As shown below, the choice of the initial distribution may have a dramatic effect on the behavior of the TP.

Taking the thermodynamic limit $N, M \to \infty$ with fixed $\rho_0 = M/N$ and using Eq. (2), we get the Fourier Laplace transform of the CGF

$$\hat{\Psi}(k;\xi) \underset{\rho_0\to0}{\sim} -2\rho_0 \frac{H(\xi)}{(1-\xi)(1+\hat{F}_1)}(1-\cos k), \tag{4}$$

where we defined $H(\xi) \equiv \sum_{x=1}^{\infty}\sum_{y=-\infty}^{\infty}\hat{F}(\mathbf{0}|x,y;\xi)$, and we used the symmetry relation $\sum_{\mathbf{Z}\neq\mathbf{0}}\hat{F}^*(\mathbf{0}|\boldsymbol{e}_1|\mathbf{Z}) = \sum_{\mathbf{Z}\neq\mathbf{0}}\hat{F}^*(\mathbf{0}|-\boldsymbol{e}_1|\mathbf{Z})$. The determination of the CGF thus amounts to the calculation of the quantities $H(\xi)$ and $\hat{F}_1$, which is detailed in the Supplemental Material [34].

Expanding $\hat{\Psi}(k;\xi)$ in powers of k from Eq. (4), focusing on the large time limit $\xi \to 1^-$, and using a Tauberian theorem [40], we get the exact expression (see the Supplemental Material [34])

$$\lim_{\rho_0\to 0}\frac{\kappa^{(2n)}(t)}{\rho_0} \underset{t\to\infty}{\sim} \frac{1}{2^{5/4}\Gamma(7/4)}t^{3/4}. \quad (5)$$

All nonzero cumulants being equal, $P_t(X)$ is a Skellam distribution [41]. In particular, the rescaled position $X_t/t^{3/8}$ is asymptotically normally distributed. Moreover, as expected, EVIs slow down the motion of the TP and result in an exponent $3/4$, intermediate between a "normal" diffusion exponent, and the single-file diffusion exponent $1/2$ [42]. The analytical predictions for the cumulants are successfully compared to results obtained from Monte Carlo simulations at intermediate times (see Fig. 2), while at long times a crossover towards a standard diffusive behavior is observed. We present below a theoretical argument that accounts for this intriguing behavior.

The key point is that the above results are derived by taking the limit $\rho_0\to 0$ before $t\to\infty$, and, to leading order, the TP does not move before being reached by a vacancy. In fact, the TP diffuses due to its interactions with the other vacancies. Therefore, in the reference frame of the TP, each vacancy experiences an additional symmetric jump probability in the x direction, denoted by $D(\rho_0)$, even on the teeth. Thus, the vacancies can jump between teeth (with a vanishing probability when $\rho_0\to 0$) and their motion is effectively two dimensional. Qualitatively, the problem is 2D and regular diffusion is expected at large times. Quantitatively, the approach developed previously can be extended (see the Supplemental Material [34]), yielding

$$\hat{\kappa}^{(2)}(\xi) = -2\rho_0\frac{\Sigma(\xi,\rho_0)(\hat{F}_1^*-\hat{F}_{-1}^*-1)}{(\hat{F}_1^*-1+\hat{F}_{-1}^*)(\hat{F}_1^*+1-\hat{F}_{-1}^*)}. \quad (6)$$

Here, $\hat{F}_{\pm1}^*\equiv\hat{F}^*(\mathbf{0}|\boldsymbol{e}_1|\boldsymbol{e}_{\pm1};\xi,\rho_0)$ and $\Sigma(\xi,\rho_0)\equiv\sum_{\mathbf{Z}\neq\mathbf{0}}\hat{F}^*(\mathbf{0}|\boldsymbol{e}_1|\mathbf{Z};\xi,\rho_0)$, with $F_t^*(\mathbf{0}|\boldsymbol{e}_1|\mathbf{Z};\rho_0)$ being the probability for a vacancy to reach the origin for the first time at time t knowing that it was at site $\boldsymbol{e}_1$ at time $t-1$ and that it started from site $\mathbf{Z}$. Relying on renewal-type equations, the first-passage time densities $\hat{F}^*$ are related to the propagators of the vacancies' random walk, which are evaluated extending the method presented in Ref. [43] to treat diffusion on inhomogeneous lattices (see the Supplemental Material [34]). It is found that

$$\lim_{t\to\infty}\frac{\kappa^{(2)}(t)}{t} \underset{\rho_0\to 0}{\propto} \rho_0\sqrt{D(\rho_0)}\ln\frac{1}{D(\rho_0)}. \quad (7)$$

This equation defines the diffusion coefficient $D(\rho_0)=\lim_{t\to\infty}[\kappa^{(2)}(t)/2t]$ self-consistently when $\rho_0\to 0$ and finally yields the variance in the ultimate regime:

$$\lim_{t\to\infty}\frac{\kappa^{(2)}(t)}{t} \underset{\rho_0\to 0}{\propto} \rho_0{}^2\left(\ln\frac{1}{\rho_0}\right)^2. \quad (8)$$

These results thus show that the limits $\rho_0\to 0$ and $t\to\infty$ do not commute [44]. However, due to a subtle coupling between EVIs and the geometrical constraints of the comb geometry, the diffusive regime displays a nonanalytical dependence on the vacancy density, checked numerically in Fig. 4 of the Supplemental Material [34]. This is markedly different from the case of homogeneous lattices where a linear behavior with ρ_0 is found [37]. In addition, the comparison between Eqs. (5) and (8) shows that the crossover time between the two regimes behaves like $t_\times\sim[\rho_0\ln(\rho_0)]^{-4}$, which can be very large for dense systems. Thus, the subdiffusive behavior of the first regime is long-lived and potentially observable in real systems [46]. We now consider several extensions.

Influence of the initial conditions.—The previous results were obtained for initially uniformly distributed vacancies. We now assume that they are initially located only on the backbone, with linear density $\rho_0^{\rm lin}$ defined as the number of vacancies divided by the backbone length. Averaging over this initial distribution in Eq. (4), it is found that (see the Supplemental Material [34])

$$\kappa^{(2n)}(t) \underset{\rho_0^{\rm lin}\to 0}{\sim} \frac{\rho_0^{\rm lin}}{2^{7/4}\Gamma(5/4)}t^{1/4}. \quad (9)$$

Consequently, the cumulants now grow as $t^{1/4}$. This analytical prediction is successfully confronted to simulations (see the inset of Fig. 2). This spectacular slowdown of the dynamics with respect to the uniform initial conditions is compatible with Eq. (5), where now ρ_0 strictly vanishes. Interestingly, in this case, $t_\times\to\infty$, so that there is no crossover to a diffusive regime.

d-dimensional comb.—The previous results can also be generalized to the case of a d-dimensional comb $\mathbf{C}_d$ [3,50,51], defined recursively: starting from $\mathbf{C}_1$ (a one-dimensional lattice), $\mathbf{C}_d$ is obtained from $\mathbf{C}_{d-1}$ by attaching

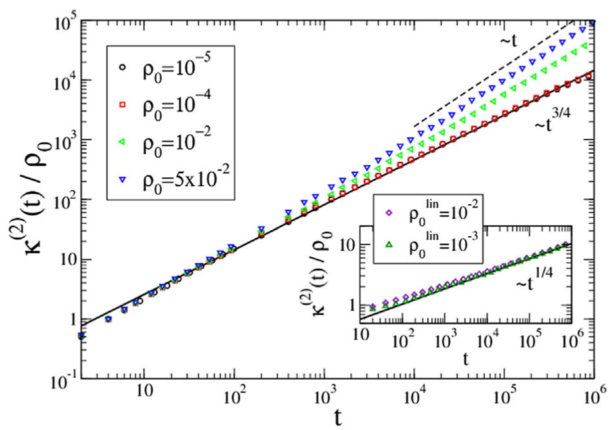

FIG. 2 (color online). Variance rescaled by ρ_0 computed from Monte Carlo simulations of vacancy dynamics. The line represents the analytical result (5). (Inset) Case where all vacancies are initially placed on the backbone [the line represents Eq. (9)].

at each point a two-way infinite path (see the figure in the Supplemental Material [34]). It is found that, for uniform initial conditions, the even cumulants all behave like

$$\lim_{\rho_0\to 0}\frac{\kappa^{(2n)}(t)}{\rho_0}\underset{t\to\infty}{\propto} t^{1-1/2^d}, \tag{10}$$

and eventually cross over to a diffusive regime for $d \geq 2$. Note that in the case $d = 1$, single-file subdiffusion $\kappa^{(2n)}(t) \propto \sqrt{t}$ is recovered.

Recalling that single-file diffusion was shown to be a realization of a fractional Brownian motion with Hurst exponent $1/4$ [52], we conjecture that tracer diffusion in a crowded d-comb with $\rho_0 \to 0$ is more generally a realization of a fractional Brownian motion of Hurst exponents $H = (2^d - 1)/2^{d+1}$.

Finally, as for the effect of initial conditions, we find that, if the vacancies are initially placed only on the backbone, $\lim_{\rho_0\to 0}\kappa^{(2n)}(t)/\rho_0 \underset{t\to\infty}{\propto} t^{1/2^d}$.

Case of a TP visiting the teeth.—We finally come back to the original problem of a tracer on a crowded 2-comb, where the TP is allowed to visit the teeth. The displacement of the TP along the backbone can be analyzed in a mean-field description that decouples the motion of the TP in a tooth from the dynamics of other bath particles as a continuous time random walk, whose waiting time distribution $\psi(t)$ describes the time the TP spends on a tooth of the crowded comb. Noting that the motion of the TP along a tooth is close to a single-file motion, we expect that the transverse MSD behaves like $\langle y^2(t)\rangle \propto \sqrt{\rho_0^2 t}$ [24] in the dense limit. In turn, this leads to two different regimes for $\psi(t)$: for $t \ll t_{\times,1} \equiv 1/\rho_0^2$, $\langle y^2(t)\rangle \ll 1$, the TP has not had time to explore a tooth because of the other bath particles, and the mean time spent on the tooth is finite; for $t \gg t_{\times,1}$, $\psi(t) \propto 1/t^{\mu}$, with $\mu = 7/4$, as obtained in Refs. [53,54] and checked numerically (see the inset of Fig. 3).

The MSD $\langle X^2\rangle$ of the TP along the backbone is then related to the MSD $\kappa^{(2)}$ of the TP restricted to the backbone by the standard Montroll-Weiss relation [40]:

$$\widehat{\langle X^2\rangle}(\xi) = \frac{1-\hat{\psi}(\xi)}{1-\xi}\widehat{\kappa^{(2)}}(\hat{\psi}(\xi)). \tag{11}$$

Combining the two temporal behaviors of $\kappa^{(2)}(t)$ determined previously with those of $\psi(t)$, we finally obtain three nontrivial regimes:

$$\langle X^2(t)\rangle \propto \begin{cases} t^{3/4} & \text{if } t \ll t_{\times,1}, \\ t^{3/4(\mu-1)} = t^{9/16} & \text{if } t_{\times,1} \ll t \ll t_{\times,2}, \\ t^{\mu-1} = t^{3/4} & \text{if } t \gg t_{\times,2}, \end{cases} \tag{12}$$

where $t_{\times,2}$ is a second crossover time (whose dependency on ρ_0 is not provided by our approach) [55]. The

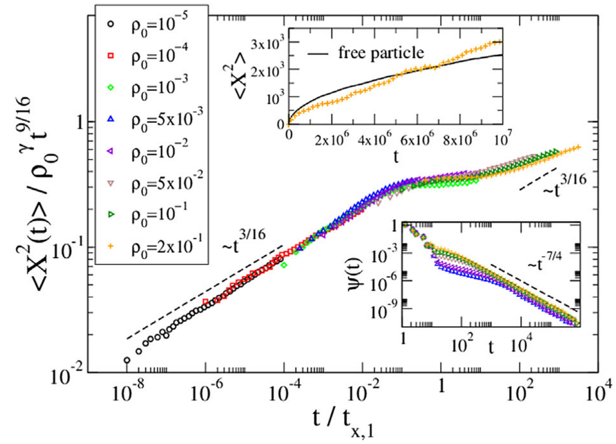

FIG. 3 (color online). Variance of the TP visiting the teeth, for different values of ρ_0. The collapse of the curves is obtained by rescaling time by $t_{\times,1} = 1/\rho_0^2$, predicted by our analytical approach, and the variance by ρ_0^{γ} with $\gamma \simeq 0.62$, numerically obtained. The plateau at intermediate times confirms the prediction of Eq. (12). For $\rho_0 \leq 10^{-3}$ the reported results are obtained via simulations of vacancy dynamics, while for $\rho_0 > 10^{-3}$ via particle dynamics (see the Supplemental Material [34]). (Top inset) Comparison with the MSD along the backbone of a free particle. (Bottom inset) Distribution of the time spent by the TP on the teeth from simulations.

comparison with numerical simulations shown in Fig. 3 reveals that (i) three regimes with expected crossover time $t_{\times,1}$ are indeed observed; (ii) the exponents of the two first are in good agreement with our analytical prediction (12); (iii) the increase of $\langle X^2(t)\rangle$ observed in the last regime is in qualitative agreement with Eq. (12), but the quantitative determination of the corresponding exponent would require more extensive simulations. Remarkably, it is found that, asymptotically, the dynamics of the TP along the backbone is faster than in the absence of bath particles, where $\langle X^2(t)\rangle \propto t^{1/2}$. In other words, the motion of the TP is accelerated along the backbone by EVIs (see the top inset of Fig. 3). A similar effect was obtained in Ref. [32], where the mobility of a single-file interacting system was shown to be increased by disorder; however, in Ref. [32], the speedup is due to disorder and only occurs at intermediate times. The surprising behavior found here results from two competing effects quantified by our approach: hard-core interactions hinder the motion of the TP along the backbone but also reduce the time lost in the teeth.

Our results show that the combined effect of geometric constraints and interactions produces intriguing behaviors. They could be relevant in different fields where such ingredients are present, like in microfluidics [56], and for transport in biological systems—e.g., in microtubules [57] or in dendritic spines [58].

The authors acknowledge financial support from the ERC Grant No. FPTOpt-277998.

[1] R. Metzler and J. Klafter, Phys. Rep. **339**, 1 (2000).
[2] S. Condamin, V. Tejedor, R. Voituriez, O. Bénichou, and J. Klafter, Proc. Natl. Acad. Sci. U.S.A. **105**, 5675 (2008).
[3] D. Ben-Avraham and S. Havlin, *Diffusion and Reactions in Fractals and Disordered Systems* (Cambridge University Press, Cambridge, England, 2005).
[4] G. Weiss and S. Havlin, Physica (Amsterdam) **134A**, 474 (1986).
[5] V. Arkhincheev and E. Baskin, Sov. Phys. JETP **73**, 161 (1991).
[6] R. Burioni and D. Cassi, J. Phys. A **38**, R45 (2005).
[7] H. Frauenrath, Prog. Polym. Sci. **30**, 325 (2005).
[8] A. Iomin, Phys. Rev. E **83**, 052106 (2011).
[9] D. Villamaina, A. Sarracino, G. Gradenigo, A. Puglisi, and A. Vulpiani, J. Stat. Mech. (2011) L01002.
[10] E. K. Lenzi, L. R. da Silva, A. A. Tateishi, M. K. Lenzi, and H. V. Ribeiro, Phys. Rev. E **87**, 012121 (2013).
[11] V. Méndez and A. Iomin, Chaos Solitons Fractals **53**, 46 (2013).
[12] E. Agliari, A. Blumen, and D. Cassi, Phys. Rev. E **89**, 052147 (2014).
[13] A. Rebenshtok and E. Barkai, Phys. Rev. E **88**, 052126 (2013).
[14] E. Agliari, F. Sartori, L. Cattivelli, and D. Cassi, Phys. Rev. E **91**, 052132 (2015).
[15] H. V. Ribeiro, A. A. Tateishi, L. G. A. Alves, R. S. Zola, and E. K. Lenzi, New J. Phys. **16**, 093050 (2014).
[16] Y. Sagi, M. Brook, I. Almog, and N. Davidson, Phys. Rev. Lett. **108**, 093002 (2012).
[17] F. Höfling and T. Franosch, Rep. Prog. Phys. **76**, 046602 (2013).
[18] T. Chou, K. Mallick, and R. K. P. Zia, Rep. Prog. Phys. **74**, 116601 (2011).
[19] E. Levine, Y. Kafri, and D. Mukamel, Phys. Rev. E **64**, 026105 (2001).
[20] H. Spohn, *Large Scale Dynamics of Interacting Particles* (Springer-Verlag, Berlin, 1991).
[21] K. Nakazato and K. Kitahara, Prog. Theor. Phys. **64**, 2261 (1980).
[22] T. Harris, J. Appl. Probab. **2**, 323 (1965).
[23] D. G. Levitt, Phys. Rev. A **8**, 3050 (1973).
[24] R. Arratia, Ann. Probab. **11**, 362 (1983).
[25] N. Leibovich and E. Barkai, Phys. Rev. E **88**, 032107 (2013).
[26] P. L. Krapivsky, K. Mallick, and T. Sadhu, Phys. Rev. Lett. **113**, 078101 (2014).
[27] C. Hegde, S. Sabhapandit, and A. Dhar, Phys. Rev. Lett. **113**, 120601 (2014).
[28] R. Burioni, D. Cassi, G. Giusiano, and S. Regina, J. Phys. A **35**, 217 (2002).
[29] O. Flomenbom and A. Taloni, Europhys. Lett. **83**, 20004 (2008).
[30] E. Barkai and R. Silbey, Phys. Rev. E **81**, 041129 (2010).
[31] L. P. Sanders, M. A. Lomholt, L. Lizana, K. Fogelmark, R. Metzler, and T. Ambjörsson, New J. Phys. **16**, 113050 (2014).
[32] E. Ben-Naim and P. L. Krapivsky, Phys. Rev. Lett. **102**, 190602 (2009).
[33] C. Amitrano, A. Bunde, and H. Stanley, J. Phys. A **18**, L923 (1985).
[34] See Supplemental Material at http://link.aps.org/supplemental/10.1103/PhysRevLett.115.220601, which includes Refs. [35,36], for details on calculations and simulations.
[35] W. Woess, *Random Walks on Infinite Graphs and Groups* (Cambridge University Press, Cambridge, England, 2000).
[36] V. E. Arkhincheev, Physica (Amsterdam) **307A**, 131 (2002).
[37] M. J. A. M. Brummelhuis and H. J. Hilhorst, Physica (Amsterdam) **156A**, 575 (1989).
[38] O. Bénichou and G. Oshanin, Phys. Rev. E **66**, 031101 (2002).
[39] P. Illien, O. Bénichou, C. Mejía-Monasterio, G. Oshanin, and R. Voituriez, Phys. Rev. Lett. **111**, 038102 (2013).
[40] B. D. Hughes, *Random Walks and Random Environments, Volume 1: Random Walks* (Oxford University, New York, 1995).
[41] J. G. Skellam, J. R. Stat. Soc. **109**, 296 (1946).
[42] Note that Eq. (5) shows that the Percus formula [30], relating the MSD in the presence of interacting particles with the average of the absolute value of the TP position in the free case, does not hold in the comb geometry.
[43] T. M. Nieuwenhuizen, S. Klumpp, and R. Lipowsky, Phys. Rev. E **69**, 061911 (2004).
[44] A similar noninversion mechanism was found in Ref. [45]. However, in contrast to what has been found here, this effect exists only when the TP experiences a nonzero bias.
[45] O. Bénichou, A. Bodrova, D. Chakraborty, P. Illien, A. Law, C. Mejía-Monasterio, G. Oshanin, and R. Voituriez, Phys. Rev. Lett. **111**, 260601 (2013).
[46] Note that these long-lived transient regimes share similarities with the phenomenon of noise-induced stability observed in metastable states [47–49].
[47] N. V. Agudov and B. Spagnolo, Phys. Rev. E **64**, 035102(R) (2001).
[48] A. Fiasconaro, B. Spagnolo, and S. Boccaletti, Phys. Rev. E **72**, 061110 (2005).
[49] A. A. Dubkov and B. Spagnolo, Phys. Rev. E **72**, 041104 (2005).
[50] D. Cassi and S. Regina, Mod. Phys. Lett. B **06**, 1397 (1992).
[51] D. Bertacchi and F. Zucca, J. Aust. Math. Soc. **75**, 325 (2003).
[52] C. Landim and S. Volchan, Stoch. Proc. Appl. **85**, 139 (2000).
[53] J. Krug, H. Kallabis, S. N. Majumdar, S. J. Cornell, A. J. Bray, and C. Sire, Phys. Rev. E **56**, 2702 (1997).
[54] G. M. Molchan, Commun. Math. Phys. **205**, 97 (1999).
[55] Notice that if the vacancies are initially placed only on the backbone, only the first regime is observable and one recovers the behavior of Eq. (9).
[56] A. Mukhopadhyay and S. Granick, Curr. Opin. Colloid Interface Sci. **6**, 423 (2001).
[57] M. A. Welte, Curr. Biol. **14**, R525 (2004).
[58] E. A. Nimchinsky, B. L. Sabatini, and K. Svoboda, Annu. Rev. Physiol. **64**, 313 (2002).